CHAPTER 2

Visual field defects and the structural brain

Part 2

Cortical thickness and visual field defects

Authors:

Christine C. Boucard

Brian T. Quinn

Nomdo M. Jansonius

Bruce Fischl

Johanna M.M. Hooymans

Frans W. Cornelissen

Submitted

Abstract

Developmental ocular disorders are known to affect the structure of visual cortex, but little is known about the effects of acquired retinal disorders. In a previous study (Boucard et al., 2006; submitted for publication), we investigated whether prolonged cortical deprivation, due to retinal field defects acquired later in life, leads to cortical changes in the adult brain. Compared to controls, we found lower grey matter (GM) concentration in the visual cortex of a group of patients suffering from glaucoma. Such a change was absent in a group of subjects with age-related macular degeneration. In order to better understand the origin of this change, we here examine cortical grey matter thickness in the same subjects. Magnetic resonance images (MRI) were obtained in subjects with glaucoma, age-related macular degeneration (AMD) and controls. Cortical thickness was compared between the groups using Freesurfer. A significant cortical grey matter thinning was found in the occipital area of the glaucoma group when compared to controls. In AMD, no difference was found. The present results corroborate and specify our previous findings. Cortical degeneration following visual deprivation later in life affects occipital cortical grey matter thickness in case of glaucoma, but not of AMD. Transneuronal degeneration, in response to the disrupted link between brain and retina caused by RGC layer loss and optic nerve damage, is discussed as the main cause of this thinning.

Introduction

Age-related macular degeneration (AMD) and glaucoma, both eye diseases associated with the occurrence of retinal visual field defects, are the two leading causes of visual impairment in the developed world (Resnikoff et al., 2004). AMD is caused by accumulated waste products in the tissues underneath the macula that interfere with retinal metabolism and lead to retinal atrophy (Holz et al., 2004; Zarbin 2004). The disease causes centrally located visual field defects. In glaucoma, where visual field loss starts peripherally and grows towards the fovea, progressive retinal ganglion cell (RGC) loss and optic nerve damage occur, in most cases induced by an elevated intra-ocular pressure (IOP) (Fetchner et al., 1994; Nickell, 1996). The major distinction between these two diseases is that the RGC and optic nerve are damaged in glaucoma but remain intact in AMD.

Due to the retinotopic cortical organisation (Inouye, 1909; Holmes et al., 1916; Dougerty et al., 2003), when field defects occur in both eyes and overlap, the retinotopic corresponding part of visual cortex is no longer stimulated. The fact that cortical tissue is affected by an absence of stimulation (Johansson, 2004; Merzenich et al., 1984) makes it pertinent to ask whether retinal field defects deteriorate the structure of the occipital cortex. Besides, this issue is highly relevant from a clinical point of view since cortical degeneration might affect functional recovery after treatment of retinal disease. Recent studies have demonstrated that developmental visual disorders such as strabismus (Chan et al., 2004), amblyopia (Mendola et al., 2005) and albinism (von dem Hagen et al., 2005) affect the structure of human occipital cortex. However, very few studies have yet examined the influence of visual deprivation later in life.

In a previous study from our group (Boucard et al., 2006; submitted for publication), we investigated this question in glaucoma and AMD. Compared to controls, in the glaucoma group a lower grey matter (GM) concentration was found in the cortical projection zone corresponding to the damaged region of the retina. At the same time, no difference was observed in the AMD group, suggesting loss of RGC and optic nerve damage to be the

essential factor for cortical degeneration to occur. This previous analysis was performed using “non-modulated” voxel-based morphometry (VBM), a technique that allows estimating differences in GM concentration in local structures between two or more groups (Ashburner et al., 2000).

Yet, the precise origin of this lower GM concentration as detected by VBM remains unclear at present. Regional GM differences assessed by VBM (namely the proportion of GM relative to other tissue types within a region) can reflect either cortical thickness differences or the effect of different amounts of folding. In addition, low voxel intensity resolution, smoothing or whole brain deformation are aspects that could lead to erroneous conclusions in VBM comparisons. In order to overcome these issues and look for corroborating evidence, we here performed a further analysis examining cortical grey matter thickness per se. The analysis was performed using the Freesurfer method (Fischl et al., 2000). With Freesurfer, cortical thickness is determined by measuring the distance between the GM/white matter (WM) boundary and the pial surface. The present analysis revealed a thinning of cortical grey matter in the lesion projection zone in the glaucoma group, while in the AMD group no such difference was found. An acquired retinal visual field defect associated with RGC layer loss and optic nerve damage can thus result in changes in the thickness of visual cortex.

Methods

Subjects

Subjects with visual field defects were recruited from a database of the Department of Ophthalmology of the University Medical Center Groningen (Groningen, The Netherlands) and through advertisements in magazines of patient associations. The group consisted of nine patients suffering from AMD (two female and seven males; mean age 73 years, range 52-82) and eight patients with primary open-angle glaucoma (one female and seven males; mean age 73 years, range 61-84). Patients had to have homonymous scotoma of at least 10 degrees diameter centrally located in at least one

quadrant. The visual field defect had to exist at least 3 years. Patients with any other (neuro-) ophthalmic disease that could affect the visual field were excluded.

In the AMD group, the homonymous visual field defects were primarily located in the foveal region, while in the glaucoma group larger peripheral visual field defects were present (although heading towards fixation due to the inclusion criterion). This difference is depicted in the visual acuity (logMAR; minimum angle of resolution) and average visual field sensitivity (MD; mean deviation) scores of both groups. Table 1 shows these characteristics.

subjects	diagnosis	visual acuity (logMAR)	visual field sensitivity (MD)	age
1	AMD	1.3	-7.6	75
2	AMD	0.7	-3.6	82
3	AMD	1	-3.5	79
4	AMD	1	-12	52
5	AMD	1	-5	82
6	AMD	0.7	-2.7	63
7	AMD	0.8	-2.6	76
8	AMD	0.4	-2.2	82
9	AMD	0.1	-4.5	68
mean	**AMD**	**0.8**	**-4.9**	**73**
10	glaucoma	0	-23	67
11	glaucoma	0.1	-13.8	69
12	glaucoma	0	-8.8	84
13	glaucoma	0.1	-5.2	82
14	glaucoma	0.7	-14.5	65
15	glaucoma	0.05	-3.7	61
16	glaucoma	0.1	-18.3	75
17	glaucoma	0.1	-6.4	80
mean	**glaucoma**	**0.1**	**-11.7**	**73**

Table 1: Subject characteristics. Visual acuity of the best eye (expressed in logMAR; minimum angle of resolution), visual field sensitivity of the best eye (expressed as the mean deviation (MD) in sensitivity (dB)) and age of the two patients group (AMD and glaucoma).

For the control group, 12 healthy age-matched subjects (three female and nine male; mean age 66 years, range 60-82) were recruited either by advertisement in a local newspaper, or were the partners of the visual field impaired participants. Control subjects were required to have good visual acuity (logMAR≤0), not to suffer from any visual field defect, and had to be free of any ophthalmic, neurologic, or general health problem.

No significant age differences between the two patient groups nor with the control group were assessed by means of t-test analysis.

This study conformed to the tenets of the Declaration of Helsinki and was approved by the medical review board of the University Medical Center Groningen (Groningen, The Netherlands). All participants gave their informed written consent prior to participation.

Materials and data acquisition

Visual fields were recorded using the Humphrey Field Analyzer (HFA; Carl Zeiss Meditec, Dublin, California, USA) running the 30-2 Sita Fast program.

High-resolution MRI was performed on a 3.0 Tesla Philips Intera (Best, The Netherlands). A 3-D structural MRI was acquired on each subject using a T1 weighted magnetization sequence T1W/3D/TFE-2, 8 degrees flip angle, matrix size 256 · 256, field of view 230.00 160.00 179.69, yielding 160 slices, voxel size 1x1x1 mm, TR 8.70 ms.

Analysis

A detailed description of the Freesurfer (http://surfer.nmr.mgh.harvard.edu/) automated procedures used here for cortical thickness measurements can be found in Fischl et al., (2000). In short, after intensity non-uniformity corrections in the MR data and Talairach normalisation, voxels are classified as WM or something else than WM based on intensity and neighbour information (Dale et al., 1999). Next, the skull is stripped using a template (Segonne et al., 2004) and a second intensity correction is performed on the brain volume. The obtained segmentations of each individual subject are visually inspected, and any obvious inaccuracies manually corrected. This is followed by an

inflation step during which metric distortion is minimized to preserve original areas and distances (Fischl et al., 1999). Finally, models are constructed of the white surface following the intensity gradients between the WM and GM, and of the pial surface according to the intensity contrast between the GM and Cerebral-Spinal Fluid (CSF) (Dale et al., 1999; Fischl et al., 2001). The distance between the white and pial surfaces defines the thickness at each location of cortex across the entire brain volume.

Statistics

Statistical maps of thickness differences were constructed using a *t* statistics. For each vertex in the cortical thickness map, group (AMD, glaucoma and controls) effects on cortical thickness were calculated using a general linear model. The participant's age was taken as a covariate factor in order to control for its potential contribution to the differences.

In the resulting statistical difference maps, thresholds were set using the false discovery rate (FDR), which corrects for the vertices that falsely show differences among those that truly display differences (Genovese et al, 2002). Our hypothesis was that as a consequence of interrupted cortical stimulation, the visual field defect groups would show lower thickness values than the control group. Because of the unidirectional nature of these expectations, we choose a FDR threshold of 0.1 (which would correspond to the commonly accepted 0.05 threshold if the hypothesis would consider the possibility of effects occurring in both directions).

The resulting regions with a significant difference in cortical thickness between groups were mapped on the mean inflated surface of all participants (figure 1).

Results

Figure 1 shows the results of the comparison of cortical thickness between the control and the glaucoma group. In both left and right hemispheres, the comparison led to lower values of cortical thickness in regions in the anterior medial part of the occipital lobe of the glaucoma group. Conversely, the analysis did not reveal any significant differences

in cortical thickness between AMD patients and controls. The cortical thickness of both groups included in these corresponding regions is displayed in figure 2.

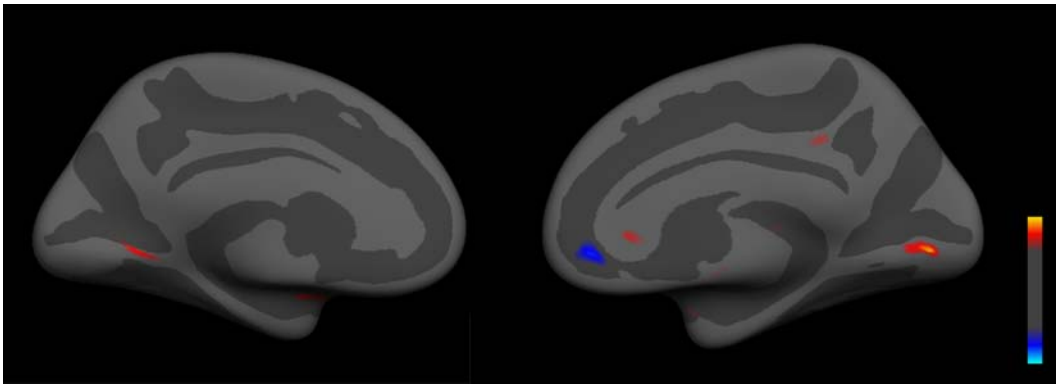

Figure 1: Results. Regions of difference in cortical thickness resulting from the comparison glaucoma<controls. The results are mapped on the mean inflated surface from all participants' brains.

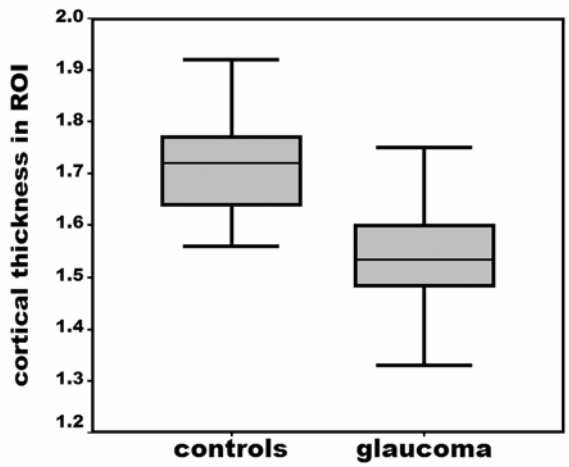

Figure 2. Results. Boxplots displaying the cortical thickness of both control and glaucoma group in the ROI resulting from the comparison controls>glaucoma. The data includes the average thickness from both left and right hemispheres.

Discussion

In this study, we observed that in comparison to a group of age-matched controls, patients with glaucoma show a local cortical thinning in the occipital region. Conversely, in the case of AMD no such differences in cortical thickness were found. These results corroborate those of a previous study in which GM concentration was compared between these groups using VBM. Hence, two substantially different types of analysis result in the same conclusion. We consider this as additional evidence for the idea that cortical degeneration is associated with acquired retinal visual field defects in glaucoma. Most likely this degeneration is a response to the disruption of the connection between brain and retina as a result of RGC and optic nerve damage.

Comparison of methods

In order to understand the value of performing an additional analysis on the same groups of subjects, we here discuss the main differences between the VBM and Freesurfer methods for evaluating structural changes.

In short, VBM identifies differences in the proportion of GM relative to other tissue types within a region. This is achieved by spatially normalising to the same stereotactic space, segmenting the normalised images into GM, WM and CSF, smoothing the segmentation of interest and finally performing a statistical analysis to localise significant differences between two or more experimental groups. However, with GM concentration, one can only measure relative amounts of GM within a region. These regional characteristics do not allow discriminating between differences in cortical thickness and differences in the amount of folding. The reason why the cortical thickness analysis was performed is to verify if the GM decrease we found using the VBM method reflects actual cortical reduction. The Freesurfer method (Dale et al., 1999; Fischl et al., 1999, Fischl et al., 2000) has been validated using post-mortem brains (Rosas et al., 2002), and manual measurements (Kuperberg et al., 2003).

Because of the brain's natural cortical folding, with VBM a direct measurement of cortical thickness is not possible. Adjacent gyri can be mistaken as a single thick GM area and be reported to show a local high GM concentration (Mechelli et al., 2005).

Instead, the surface-based approach in Freesurfer allows following exactly the GM/WM boundary and pial surfaces avoiding possible errors coming from the folded structure. The result is an accurate approximation about how the cortical ribbon appears in real.

During the voxel classification process, VBM assigns to each voxel a specific brain tissue (GM, WM and CSF) according to its intensity and location. In order to construct a GM segmented volume that can be used in the final statistical comparison, the segmentation algorithm is required to detect intensity variations very precisely. Estimation on the basis of absolute intensity can easily result in segmentation errors. For example, a voxel containing only WM and CSF could erroneously be classified as GM because of its average intensity. A slightly different approach is used in Freesurfer (Fischl et al., 2000) that avoids this kind of segmentation errors. First, a WM volume is created by classifying voxels as WM or something else than WM based on intensity and neighbour constraints. Then, using intensity contrast information, models of the boundary GM/WM as well as the pial surface (GM/CSF boundary) are constructed (Dale et al., 1999). Because cortical thickness is defined as the shortest distance between these two surfaces models, the GM volume model does not result from specific classifications depending on voxel intensities and is independent of voxel resolution. As a consequence, GM comparisons are directly linked to the cortical ribbon enabling a more accurate approximation of reality.

Another issue suggesting that Freesurfer's modelling of the GM is more in agreement with reality is the fact that thickness measures are independent of any smoothing. On the contrary, in VBM, in order to compensate for inaccuracies in the normalisation process, the segmented data are smoothed. While this can induce mistakes in the localisation of differences, the Freesurfer analysis permits to exactly locate thickness differences. Besides, since the maps are not restricted to the voxel resolution of the original data, the detection of submillimeter differences between groups is possible (Fischl et al., 2000).

The VBM normalisation process only fits the overall brain shapes. Changes detected by this method can be dramatically influenced by possible whole brain deformation. Consider as an example the case where GM atrophy occurs on the parietal temporal border. This could cause the brain to shrink in that area pulling the parietal region and

the occipital lobe towards the void created by the atrophy. This could subsequently enlarge the gap between the left and right occipital lobes which consequently could be detected as a region of lower GM concentration by VBM. When directly investigating cortical thickness, as with Freesurfer, this cannot be the case.

Discussion of results

The region with diminished cortical thickness in the glaucoma group is located in the medial anterior occipital lobe. The location is in accordance with the cortical projection zone associated with loss of peripheral retinal input (Inouye, 1909; Holmes et al., 1916; Dougerty et al., 2003). The fact that the field defects of the glaucoma group had a more peripheral location supports the idea that cortical thinning is specifically associated with the field defect. Our results therefore indicate that an acquired retinal visual field defect can lead to selective atrophy in the visual cortex.

Taking into account that in AMD field defects are located in the foveal region, a similar thinning in more posterior occipital regions would have been expected if an absence of normal stimulation is the underlying cause. One could argue that the reason why no cortical thinning was detected was that the extent of the field defect was not as large as in the glaucoma group, where it covered not only the centre but also part of the periphery of the visual field. But, as a result of cortical magnification the foveal region is overrepresented in visual cortex, so the expected corresponding cortical lesion should still be considerable.

Another argument could be that in the AMD group the severity of the retinal field defect was less pronounced than in the glaucoma group (see table 1, visual field sensitivity). Although one could think that only the more severe degeneration associated with glaucoma has been detected, the fact that RGC and optic nerve damage occurs in glaucoma but is absent in AMD is more likely to explain the difference in cortical thickness. There is strong evidence linking optic nerve damage and atrophy in visual cortex. For example, from animal studies, it is known that retinal and optic nerve lesions produce histological changes in the visual pathway (Haddock et al., 1950). Furthermore, enucleation in monkeys leads to neuronal loss in lateral geniculate nucleus (LGN) and striate cortex (Haseltine et al., 1979). Visual deprivation in postnatal life results in a

decay of visual cortical neurons as well (Nucci et al., 2003, Tigges et al., 1984). Moreover, induced glaucoma using experimentally elevated IOP in cats (Chen et al., 2003) and non-human primates (Yucel et al., 2003) causes cell reduction in LGN and visual cortex. In post-mortem human brains, a strong correlation was found between the size of the LGN and visual cortex and the size of optic nerves and tracts (Andrews et al., 1997).

Another finding supporting the idea that differences in RGC and optic nerve damage are the main causal factor in explaining the presence or absence of atrophy in our groups comes from a recent neuro-imaging study. In this study, in human albinos a reduced optic nerve and visual cortex were found (Von Dem Hagen et al., 2005). In albinism, RGC density in the central retina is significantly reduced (Guillery et al., 1984). This, in addition to our findings, suggests that cortical degeneration may occur irrespective of the retinal location of the atrophic area and is mainly a consequence of RGC damage.

By transneuronal degeneration the atrophy from damaged parts of the retina can propagate towards the cortex provoking its atrophy. This has been shown, for example, in cats and monkeys where the retina was experimentally injured by an induced elevated IOP (Chen et al., 2003; Gupta et al., 2003). Because of the presence of optic nerve damage in the glaucoma group, we consider transneuronal degeneration as the main mechanism responsible for cortical thinning.

In the case of the AMD group, degeneration of neurons in visual cortex could be prevented by the intact RGC layer producing spontaneous activity. Evoked potentials have been measured in the rabbit visual cortex after electrical stimulation of the eye in which the photoreceptor layer had been experimentally destroyed (Humayun et al., 1995).

Besides, in recent papers, large-scale functional reorganisation in visual cortex was described in two subjects suffering from AMD (Baker et al., 2005), whereas experimentally induced scotoma that included destruction of the RGC layer in the peripheral visual field of macaque monkeys showed no sign of reorganisation after seven months (Smirnakis et al., 2005). These two studies suggest that the existence of a functioning RGC correlates with the occurrence of reorganisation in visual cortex.

This, in turn, is consistent with the idea that cortical thinning occurs only when visual cortex is isolated from the retina as happens in the case of optic nerve damage.
Finally, the correspondence between the results we obtained by using the two methods strongly suggests that the lower GM concentrations found in the glaucoma group are a consequence of cortical thinning. However, a common observation that is valid for both methods is that it is not clear if the observed cortical changes (GM concentration as well as cortical thickness) originate from neuronal loss or reflect other kind of alterations such as changes in neuronal size, neuropil, dendritic or axonal arborisation. Unfortunately, this issue can only be investigated by methods other than MRI (Mechelli et al., 2005).

In conclusion, using a method that calculates cortical thickness, we corroborate and extend the findings of our previous study demonstrating a decreased GM concentration in glaucoma compared to age-matched controls. We now show that these lower GM concentrations are indeed a consequence of cortical thinning. Hence, occipital cortical thinning can be observed in visual cortex following retinal visual field defects acquired later in life. Previous studies and the absence of cortical atrophy in subjects with AMD suggest that cortical thinning results from transneuronal degeneration following loss of RGCs. This study thus contributes as well to understanding brain plasticity at later age in general.
In the clinical point of view, a better understanding of the relation between retinal visual field defects and structural changes in visual cortex may help understand disease symptoms as well as their progression. Cortical degeneration may limit the efficacy of rehabilitation and training programs (Safran et al., 1996), retinal prostheses (Hossain et al., 2005), and may require new therapeutic strategies (Taub et al., 2002) to prevent blindness.

Acknowledgement

C.C.B. is supported by an Ubbo Emmius grant from the University of Groningen, The Netherlands. A visit of C.C.B. to the Athinoula A Martinos Center was additionally supported by a grant from the Prof. Mulder foundation. Support for this research at the Athinoula A Martinos Center was provided in part by the National Center for Research Resources (P41-RR14075, R01 RR16594-01A1 and the NCRR BIRN Morphometric Project BIRN002, U24 RR021382), the National Institute for Biomedical Imaging and Bioengineering (R01 EB001550) as well as the Mental Illness and Neuroscience Discovery (MIND) Institute. We thank Paul Maguire for suggesting the cortical thickness measure in addition to the grey matter concentration and for his guidance in the data analysis. We also thank Martin Pavlovsky for his contribution to the discussion about the methodology.

References

1. Andrews TJ, Halpern SD, Purves D. Correlated size variations in human visual cortex, lateral geniculate nucleus, and optic tract. J Neurosci 1997; 17: 2859-2868.
2. Ashburner J, Friston KJ. Voxel-based morphometry--the methods. Neuroimage 2000; 11: 805-821.
3. Baker CI, Peli E, Knouf N, Kanwisher NG. Reorganization of visual processing in macular degeneration. J Neurosci 2005; 25: 614-618.
4. Chan ST, Tang KW, Lam KC, Chan LK, Mendola JD, Kwong KK. Neuroanatomy of adult strabismus: a voxel-based morphometric analysis of magnetic resonance structural scans. Neuroimage 2004; 22: 986-994.
5. Chen X, Sun C, Huang L, Shou T. Selective loss of orientation column maps in visual cortex during brief elevation of intraocular pressure. Invest Ophthalmol Vis Sci 2003; 44: 435-441.
6. Dale AM, Fischl B, Sereno MI. Cortical surface-based analysis. I. Segmentation and surface reconstruction. Neuroimage 1999; 9: 179-194.
7. dem Hagen EA, Houston GC, Hoffmann MB, Jeffery G, Morland AB. Retinal abnormalities in human albinism translate into a reduction of grey matter in the occipital cortex. Eur J Neurosci 2005; 22: 2475-2480.
8. Dougherty RF, Koch VM, Brewer AA, Fischer B, Modersitzki J, Wandell BA. Visual field representations and locations of visual areas V1/2/3 in human visual cortex. J Vis 2003; 3: 586-598.
9. Fechtner RD, Weinreb RN. Mechanisms of optic nerve damage in primary open angle glaucoma. Surv Ophthalmol 1994; 39: 23-42.
10. Fischl B, Sereno MI, Dale AM. Cortical surface-based analysis. II: Inflation, flattening, and a surface-based coordinate system. Neuroimage 1999; 9: 195-207.
11. Fischl B, Dale AM. Measuring the thickness of the human cerebral cortex from magnetic resonance images. Proc Natl Acad Sci U S A 2000; 97: 11050-11055.
12. Fischl B, Liu A, Dale AM. Automated manifold surgery: constructing geometrically accurate and topologically correct models of the human cerebral cortex. IEEE Trans Med Imaging 2001; 20: 70-80.
13. Genovese CR, Lazar NA, Nichols T. Thresholding of statistical maps in functional neuroimaging using the false discovery rate. Neuroimage 2002; 15: 870-878.
14. Guillery RW, Hickey TL, Kaas JH, Felleman DJ, DeBruyn EJ, Sparks DL. Abnormal central visual pathways in the brain of an albino green monkey (Cercopithecus aethiops). J Comp Neurol 1984; 226: 165-183.
15. Gupta N, Yucel YH. Brain changes in glaucoma. Eur J Ophthalmol 2003; 13 Suppl 3: S32-S35.
16. HADDOCK JN, BERLIN L. Transsynaptic degeneration in the visual system; report of a case. Arch Neurol Psychiatry 1950; 64: 66-73.
17. Haseltine EC, DeBruyn EJ, Casagrande VA. Demonstration of ocular dominance columns in Nissl-stained sections of monkey visual cortex following enucleation. Brain Res 1979; 176: 153-158.
18. Holmes G, Lister WT. Disturbances of vision from cerebral lesions with special reference to the macula. Brain 1916; 39: 34-73.
19. Holz FG, Pauleikhoff D, Klein R, Bird AC. Pathogenesis of lesions in late age-related macular disease. Am J Ophthalmol 2004; 137: 504-510.
20. Hossain P, Seetho IW, Browning AC, Amoaku WM. Artificial means for restoring vision. BMJ 2005; 330: 30-33.
21. Humayun M, Sato Y, Propst R, de Juan E Jr. Can potentials from the visual cortex be elicited electrically despite severe retinal degeneration and a markedly reduced electroretinogram? Ger J Ophthalmol 1995; 4: 57-64.
22. Inouye T. Die Sehstorungen bei Schussverletzungen der kortikalen Sehsphare nach Beobachtungen an Verwundeten der letzten japanischen Kriege. Leipzig: W Engelmann 1909.
23. Johansson BB. Brain plasticity in health and disease. Keio J Med 2004; 53: 231-246.
24. Kuperberg GR, Broome MR, McGuire PK, David AS, Eddy M, Ozawa F et al. Regionally localized thinning of the cerebral cortex in

schizophrenia. Arch Gen Psychiatry 2003; 60: 878-888.

25. Mechelli A, Price CJ, Friston KJ, Ashburner J. Voxel-Based Morphometry of the Human Brain: Methods and Applications. Current Medical Imaging Reviews 2005; 1: 105-113.
26. Mendola JD, Conner IP, Roy A, Chan ST, Schwartz TL, Odom JV et al. Voxel-based analysis of MRI detects abnormal visual cortex in children and adults with amblyopia. Hum Brain Mapp 2005; 25: 222-236.
27. Merzenich MM, Nelson RJ, Stryker MP, Cynader MS, Schoppmann A, Zook JM. Somatosensory cortical map changes following digit amputation in adult monkeys. J Comp Neurol 1984; 224: 591-605.
28. Nickells RW. Retinal ganglion cell death in glaucoma: the how, the why, and the maybe. J Glaucoma 1996; 5: 345-356.
29. Nucci C, Piccirilli S, Nistico R, Morrone LA, Cerulli L, Bagetta G. Apoptosis in the mechanisms of neuronal plasticity in the developing visual system. Eur J Ophthalmol 2003; 13 Suppl 3: S36-S43.
30. Resnikoff S, Pascolini D, Etya'ale D, Kocur I, Pararajasegaram R, Pokharel GP et al. Global data on visual impairment in the year 2002. Bull World Health Organ 2004; 82: 844-851.
31. Rosas HD, Hevelone ND, Zaleta AK, Greve DN, Salat DH, Fischl B. Regional cortical thinning in preclinical Huntington disease and its relationship to cognition. Neurology 2005; 65: 745-747.
32. Safran AB, Landis T. Plasticity in the adult visual cortex: implications for the diagnosis of visual field defects and visual rehabilitation. Curr Opin Ophthalmol 1996; 7: 53-64.
33. Segonne F, Dale AM, Busa E, Glessner M, Salat D, Hahn HK et al. A hybrid approach to the skull stripping problem in MRI. Neuroimage 2004; 22: 1060-1075.
34. Smirnakis SM, Brewer AA, Schmid MC, Tolias AS, Schuz A, Augath M et al. Lack of long-term cortical reorganization after macaque retinal lesions. Nature 2005; 435: 300-307.
35. Taub E, Uswatte G, Elbert T. New treatments in neurorehabilitation founded on basic research. Nat Rev Neurosci 2002; 3: 228-236.
36. Tigges M, Hendrickson AE, Tigges J. Anatomical consequences of long-term monocular eyelid closure on lateral geniculate nucleus and striate cortex in squirrel monkey. J Comp Neurol 1984; 227: 1-13.
37. Yucel YH, Zhang Q, Weinreb RN, Kaufman PL, Gupta N. Effects of retinal ganglion cell loss on magno-, parvo-, koniocellular pathways in the lateral geniculate nucleus and visual cortex in glaucoma. Prog Retin Eye Res 2003; 22: 465-481.
38. Zarbin MA. Current concepts in the pathogenesis of age-related macular degeneration. Arch Ophthalmol 2004; 122: 598-614